JOURNAL OF APPLIED ELECTROCHEMISTRY 19 (1989) 239–246

Cyclic chronopotentiometric studies of the LiAl anode in methyl acetate

Y. S. FUNG, H. C. LAI

Department of Chemistry, University of Hong Kong, Hong Kong

Received 15 March 1988; revised 27 May 1988

The applicability of methyl acetate as a solvent for ambient temperature lithium secondary batteries was investigated using cyclic chronopotentiometry. Methyl acetate was found to be stable towards lithium–aluminium alloys and cycling up to more than 300 cycles was obtained with about 90% cycling efficiency. Water and other organic impurities have been identified in methyl acetate and a thorough purification procedure has been used to reduce these to acceptable levels. $LiAsF_6$, $LiPF_6$, $LiClO_4$ and $LiBF_4$ were investigated for use as supporting electrolytes and $LiAsF_6$ was found to be the best in terms of cycling efficiency, longer cycling numbers and yielding the lowest corrosion capacity loss rate. The development of the LiAl anode upon cycling was observed in parallel with the reduction in nucleation polarization potential, the increase in cycling efficiency, the lowering of concentration polarization at the electrode surface and the more ready acceptance of lithium deposition at the developed electrode. The optimum conditions for the development of the LiAl anode were found to exist at a current density of $5\,mA\,cm^{-2}$ and a charge density of $0.5\,C\,cm^{-2}$.

1. Introduction

Various organic solvents have undergone active investigation in recent years for use in secondary ambient temperature lithium batteries with regard to the stability towards lithium, the commercial availability in large quantities with reliable supply and the ability to operate at low temperatures. A large variety of aprotic organic solvents have been studied such as propylene carbonate (PC) [1–9], γ-lactone-based electrolytes [10], 1,3-dioxolane [11, 12], tetrahydrofuran (THF) [13–15], 2-methyltetrahydrofuran (2-MeTHF) [16, 17], methyl acetate (MA) [18, 19] and dimethoxyethane (DME) [20]. The solvents may be used alone or mixed together to provide suitable viscosity, conductivity and inertness towards lithium [20].

The major problem facing the use of an organic solvent is the reactivity towards lithium, leading to the formation of undesirable side products and passivation of the lithium anode [21, 22]. PC was shown to be decomposed by lithium to propene [23], acetonitrile had been broken into a number of products liberating methane [24], THF reacted with lithium to form various ring-opened products [14, 16] and the 1,3-dioxolane/$LiClO_4$ system was shown to have a tendency to detonate and explode during cycling [11].

Three methods are currently used to reduce the reaction between the lithium anode and the organic solvent. The first method is to reduce the activity of lithium by alloying it with suitable substrates such as aluminium [25], though with a loss of 0.4 V in cell voltage. The second method is to use specially purified solvents to cut down the corrosion due to the more reactive impurities present in the solvent. The third method is via the formation of a barrier type coating between the electrolyte and the lithium so as to reduce its interaction with the solvent. The most successful example for this is the use of $LiAsF_6$ as the supporting electrolyte [14] in the lithium organic cell.

Of the organic solvents investigated, methyl acetate, a simple aliphatic ester, is the least studied. Only preliminary cycling with lithium metal had been carried out [18, 19]. It has been shown in our preliminary studies to be stable towards lithium, much less hygroscopic compared to other organic solvents [18], cheap and with abundant supply commercially, and with the capability of being purified easily by distillation. Thus, a more detailed investigation on the use of methyl acetate as a solvent for lithium batteries has been conducted in the present study using the three methods described above to reduce the interaction between the alkali metal alloys and the organic solvent. The technique of cyclic chronopotentiometry was used in the present study as it closely resembles actual battery operation and the interaction between the solvent and the anode can be studied over a longer period of time under cycling. The results obtained provide the information needed for the evaluation of methyl acetate as solvent or co-solvent for ambient temperature lithium batteries.

2. Experimental details

2.1. *Electrolyte and electrode preparation*

The lithium salts used as supporting electrolyte were obtained from various suppliers as shown below: $LiClO_4$ (BDH, dry), $LiAsF_6$ (Alfa), $LiPF_6$ (Alfa) and $LiBF_4$ (Alfa). $LiClO_4$ was firstly ground to a fine powder and dried under vacuum at 160° C for 48 h.

0021-891X/89 $03.00 + .12

The dried salt was ground again in a dry glove box under positive pressure of the inert gas. $LiAsF_6$, $LiPF_6$ and $LiBF_4$ were packed under argon atmosphere when received. They were used directly without further treatment in the dry box. Results of the Karl Fischer analysis showed that the electrolytes prepared above contained water less than 100 ppm. The water content in the electrolyte could be further lowered down to 50 ppm by passing the electrolyte through several columns of pre-dried 4 Å molecular sieve inside the dry glove box.

A Ag/Ag^+ (0.1 M $AgNO_3$ in acetonitrile) electrode was used as the reference electrode throughout the study. The equilibrium potential of this electrode was found to be +3.32 V with respect to the Li^+/Li electrode. All potential measurements reported in the present work were scaled back to the Li^+/Li couple for easy comparison. A lithium wire cut from lithium rod (BDH, 99.9%) to the dimensions 30 mm long and 4 mm in diameter was used as the counter electrode. The working electrode was either an aluminium wire (BDH, 99.9%), diameter 0.705 mm or a nickel wire (BDH, S.W.G. 36), diameter 0.187 mm. All working electrodes used were prepared by firstly degreasing with acetone, then mechanically polishing to a mirror finish using alumina powder, and finally cleaned by immersion in methyl acetate in an ultrasonic bath to avoid water contamination. The electrode was then dried in a stream of argon before use. The experiments were performed in the cell under a slight positive pressure of argon inside the dry box.

2.2. *Purification of the organic solvents*

Methyl acetate (Merck) was purified firstly by shaking with anhydrous potassium carbonate to remove acidic impurities. Trace amounts of methanol in the solvent were removed by conversion to methyl acetate after refluxing for 6 h with acetic anhydride (85 ml l^{-1}), followed by fractional distillation. The distillate was then refluxed and distilled with phosphorus pentoxide under an argon atmosphere to reduce the moisture content. Only the middle 60% fraction was collected. Finally, pre-dried molecular sieve (Merck, 4 Å) was added to the purified solvent to further reduce the residual level of water.

Propylene carbonate, 2-methyl tetrahydrofuran and acetonitrile were purified by distillation and dried over molecular sieve 4 Å before use. To avoid decomposition at high boiling temperature (241° C), PC was distilled under vacuum. In addition to the above, 2-methyl tetrahydrofuran was distilled with benzophenone to remove trace amounts of peroxide in the solvent. To reduce contamination, all preparative work was conducted and all solvents were stored under an argon atmosphere after treatment in the dry glove box.

2.3. *Apparatus*

A Princeton Applied Research 363 Potentiostat/Galvanostat was used to provide constant current for the chronopotentiometric studies. The voltage output was recorded using a Houston Instruments Omniscribe *Y–t* recorder. For the galvanostatic cycling studies, the plating time was controlled by the timing modules of the Chemical Electronics Model 01 Waveform Generator which was connected to a self-constructed electronic automatic switching unit [26]. The action of the automatic switching unit was controlled by the timing trigger at one end and the voltage comparator coupled with potential buffer at the other end to provide switching at required time and potential.

The concentration of lithium in the spent electrode for cycling efficiency studies was determined by atomic absorption spectrophotometry after dissolution of the anode in 20 ml conc. HCl with the addition of a trace amount of mercuric chloride to catalyse the reaction. Potassium nitrate was added so that the final solution (50 ml) would contain 2000 $\mu g\,ml^{-1}$ potassium. A Varian Techtron Model 1200 Atomic absorption Spectrophotometer equipped with a flame atomizer was used for the determination using lithium carbonate to make up the standard solution. Air/acetylene was used as the flame and 670.8 nm was selected as the absorption wavelength with 0.5 nm spectral band width.

The specific conductances of various electrolytes were measured at 25° C using a Radiometer Conductivity meter-type CDM 2C calibrated against 0.1 M aqueous KCl standard. The impurities in methyl acetate were analysed using a Varian Aerograph Model 1860-4 Gas Chromatograph. The moisture contents of the purified solvents were determined using Metrohm Herisau Karl-Fischer Model E547 Autotitrator equipped with the Multi-Dosimat E415 and Multi-Burette E485 for automatic determination of the end point of the Karl-Fischer titration using the amperometric method.

3. Results and discussion

3.1. *Preliminary studies*

The chemical reactivity of lithium towards methyl acetate was studied using the wet standing method. Strips of freshly cut lithium metal were immersed in 1 M $LiClO_4$ solutions of methyl acetate (MA), propylene carbonate (PC), 2-methyl tetrahydrofuran (2Me-THF) and acetonitrile (AN) in four individual sample tubes sealed under argon atmosphere. The change in appearance was observed over a period of 3 weeks. The results shown in Table 1 indicate that the chemical stabilities of 2Me-THF and AN towards lithium were poor while MA and PC are fairly stable in contact with lithium metal.

As the visual stability may be due to the formation of an insoluble passivated film [1], cyclic chronopotentiometric tests were performed using the four solvent systems at a constant current density of 5 mA cm^{-2} and a plating charge density of 0.5 C cm^{-2} per cycle. The results are shown in Fig. 1. In general, the results

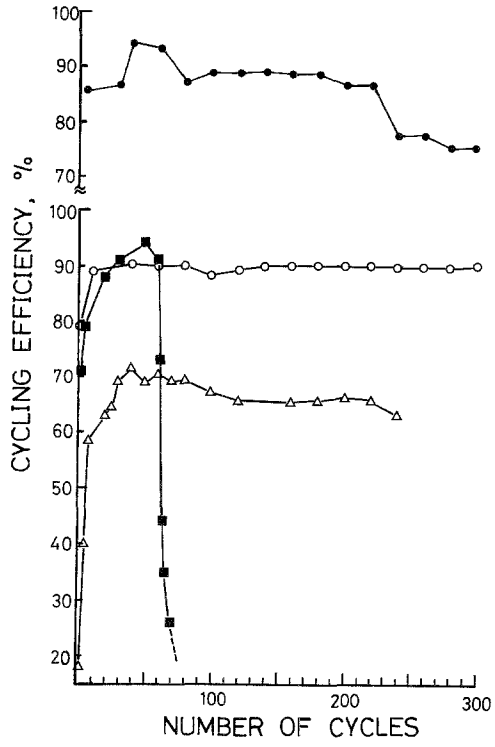

Fig. 1. Investigation of the variation of cycling efficiencies using various organic solvents: ● PC/1 M $LiClO_4$, ○ MA/1 M $LiClO_4$, ■ 2Me-THF/1 M $LiClO_4$, △ AN/1 M $LiClO_4$. Working electrode: Al, 0.56 cm^2; c.d.: 5 mA cm^{-2}.

follow the same trend as the visual observations. AN shows a low cycling efficiency at all cycles, whereas 2Me-THF exhibits a premature drop in the efficiencies when cycling more than 50 cycles, though the cycling efficiency can be as high as 94% in the first 50 cycles. This may be due to the formation of peroxide, a well-known phenomenon as a result of the decomposition of cyclic ether due to heat, light, air and moisture upon storage. As a matter of fact, ethyl peroxides which were originally absent in the electrolyte were detected in the final solutions by means of freshly prepared 10% potassium iodide solution.

In general, the cycling behaviour of MA is comparable, if not better, than that of PC. A cycling efficiency of 90% is always obtained up to 300 cycles. As it is available commercially with reliability of supply, is relatively cheap, with high specific conductance, low viscosity and is easy to purify by distillation, a more detailed investigation using the cyclic chronopotentiometric technique was conducted to investigate its applicability for ambient temperature secondary lithium batteries.

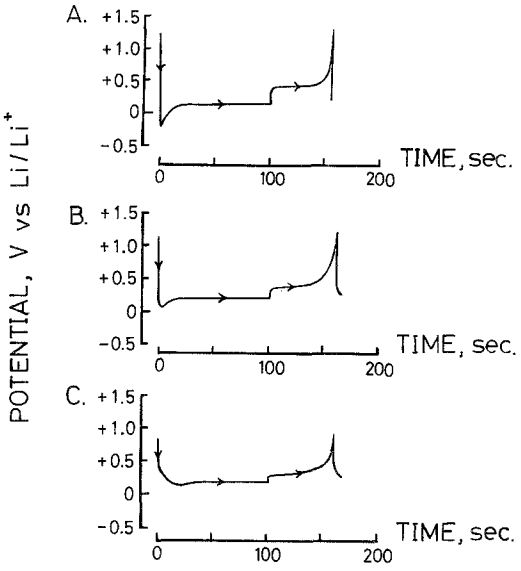

Fig. 2. Cyclic chronopotentiograms of LiAl anode in methyl acetate at different cycles. Working electrode: Al, 0.56 cm^2; c.d.: 2.5 mA cm^{-2}. (A) 1st cycle, (B) 10th cycle, (C) 250th cycle.

3.2. *General aspects of cyclic chronopotentiometric studies*

The cyclic chronopotentiograms for the deposition and stripping of lithium from aluminium in MA are shown in Fig. 2 for the 1st, 10th and 250th cycles. As only one potential plateau was observed for the formation of lithium-rich phases at the aluminium electrode surface during lithium deposition, the charging process is controlled by a pre-set time, whereas the discharge was limited by a pre-set potential at + 2.3 V with respect to Li/Li^+ couple.

As shown in Fig. 2, during the deposition of lithium, a potential spike was observed at the beginning, indicating the occurrence of nucleation polarization during the onset of the β phase at the α-Al electrode surface. No corresponding potential spike was observed during the stripping process, as no phase change occurred at the beginning of the discharging process. However, a notable potential difference was observed between the charging and the discharging plateaus, especially during the first cycle (Fig. 2). The potential difference may be due to the internal resistance of the cell or correspond to different lithium activities in the β phase at the surface of the electrode during charging and discharging. The latter may be the major factor, as the potential difference decreases rapidly with the number of cycles (Fig. 2), indicating

Table 1. Visual observations of the reactivities of various electrolytes in contact with lithium

Electrolytes	*Lapsed time before observation*			
	30 min	*1 day*	*1 week*	*3 weeks*
1 M $LiClO_4$/MA	No change	No change	No change	Dull Li surface
1 M $LiClO_4$/PC	No change	No change	No change	Dull Li surface
1 M $LiClO_4$/2Me-THF	No change	Dull Li surface	Yellowish solution	Yellowish solution
1 M $LiClO_4$/AN	Reddish brown film on Li	Whole solution dark brown	Whole solution gelled	Whole solution gelled

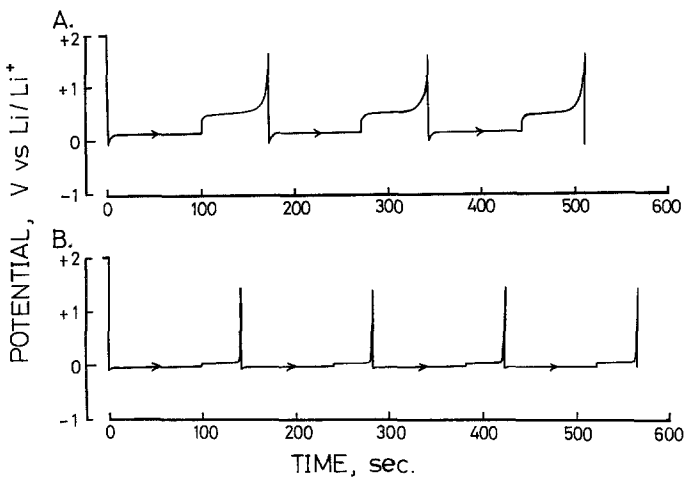

Fig. 3. Cyclic chronopotentiograms of lithium deposition on different substrates. (A) Aluminium, c.d.: 5 mA cm^{-2}, started in 1st cycle. (B) Nickel, c.d.: 5 mA cm^{-2}, started in 1st cycle.

the development of the electrode to accept more lithium at reduced concentration gradients upon cycling. The potential spike was also shown to decrease upon cycling as a result of the above development, making the nucleation of the β phase much easier at a developed electrode.

The relative contribution of resistance and concentration (of lithium at electrode surface) polarization was further illustrated in Fig. 3 using alloyed and inert substrates for the deposition of lithium. In an inert substrate like nickel, the difference in potential between the two plateaus is mainly due to the resistance polarization, which is very small as compared to the alloyed substrate using aluminium with the same c.d. A small but clear potential spike was also observed for the inert substrate during the onset of nucleation of lithium metal at the nickel substrate, another indication of the nucleation polarization of metal deposited on a foreign substrate.

3.3. *Change of coulombic efficiency upon cycling*

The change of coulombic efficiency upon cycling is affected by the c.d., number of cycles and the charge densities. The effect of c.d. is shown in Figs 4 and 5. The first few cyles are always different from the rest, during which the cycling efficiency increases rapidly until a steady value is obtained (Fig. 4). This indicates that a certain intake of lithium is required for the development of the electrode. The same fact is also borne out by the determination of coulombic efficiencies based on the lithium content analysed by atomic absorption spectrophotometry after the first cycle (Table 2). Comparing results with Fig. 5, it is clear that the lithium determined at the spent electrode by analysis is always higher than the strippable lithium obtained by coulombic calculation. Thus, some lithium must be retained by the electrode during the initial few cycles.

An optimum c.d. of 5 mA cm^{-2} was obtained (Fig. 5) with cycling efficiency at 90% for a fully developed electrode. The deviation of cycling efficiency from 100% is mainly due to the interaction between lithium and methyl acetate. The decreased cycling efficiency at low c.d. is due to the extra contact time between the lithium alloys and the solvent during the charging cycles. The drop of cycling efficiency at high c.d. is the result of the formation of a more corrosive lithium-rich intermetallic compound at the electrode surface as a consequence of increasing the concentration gradient to meet the required diffusion rate of lithium imposed by the constant current of the galvanostat. The high interaction rate between lithium-rich alloys with methyl acetate is clearly demonstrated by the drastic drop in cyclic efficiency using nickel as the substrate (Fig. 4) which does not alloy as readily with lithium.

The effect of charge density is shown in Fig. 6. The c.d. used is 5 mA cm^{-2} and the charge density is controlled by the imposed charging time. The result indicates that the charge density should not be higher than 2.5 C cm^{-2} during plating, otherwise the coulombic efficiency would drop rapidly upon cycling.

Table 2. The coulombic efficiency of lithium deposition on aluminium substrates at various current densities using atomic absorption spectrophotometry

Current densities (mA cm^{-2})	*Coulombs passed (10^{-3} C)*	*Lithium deposited by calculation (10^{-6} mole)*	*Lithium deposited by AAS (10^{-6} mole)*	*Coulombic efficiencies (%)*
17.9	3000	31.1	29.3	94.2
12.5	2940	30.5	29.0	95.1
8.9	3000	31.1	29.7	95.5
5.4	2970	30.8	30.0	97.4
4.5	3000	31.1	29.9	96.1
1.8	3000	31.1	26.9	86.5
0.9	3000	31.1	25.0	80.4

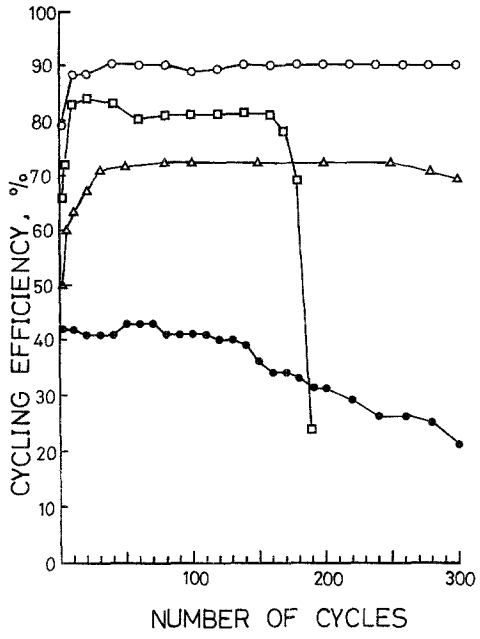

Fig. 4. The variation of cyling efficiency upon cycling at different current densities. △ 1.0 mA cm^{-2} (on Al), ○ 5.0 mA cm^{-2} (on Al), □ 12.5 mA cm^{-2} (on Al), ● 5.0 mA cm^{-2} (on Ni).

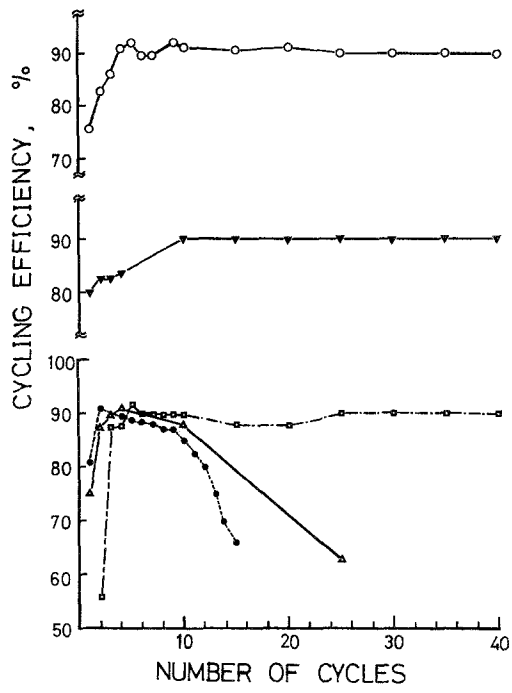

Fig. 6. The variation of cycling efficiency upon cycling at various charge densities. Working electrode: Al, 0.45 cm^2; c.d.: 5 mA cm^{-2}. ○ 0.05 C cm^{-2}, □ 0.25 C cm^{-2}, ▼ 0.50 C cm^{-2}, △ 2.50 C cm^{-2}, ● 5.00 C cm^{-2}.

3.4. *Development of the LiAl anode*

The aluminium electrode is shown to develop upon cycling in the previous section. The development leads to a decrease in nucleation polarization of the β phase, a reduction in the concentration polarization at the lithium anode during charge and discharge cycles, an increase in cycling efficiency for the first few cycles to a steady value and a more ready acceptance of lithium at the developed electrode.

Corresponding development of the morphology of the electrode was also observed upon cycling [26]. Various degrees of expansion of the electrode were observed, dependent on the c.d., charge density and number of cycles. A current density of 5 mA cm^{-2} gave the best development as no cracking of the electrode was observed after more than 300 cycles. A charge density of 0.50 C cm^{-2} (c.d. 5 mA cm^{-2}) gave a uniform internal development with a well-defined penetrating structure of the LiAl alloys starting at the surface and extending into the interior of the electrode.

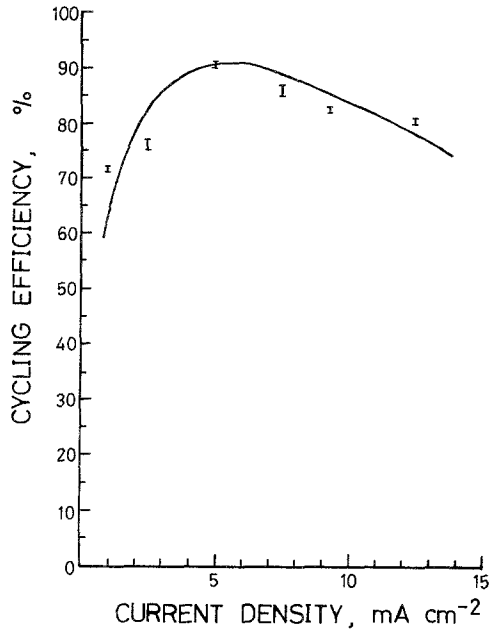

Fig. 5. The effect of current density on cycling efficiency at steady state.

As the crystal structure of the α phase (FCC, a = 0.404 nm) is distinctly different from that of the β phase (NaTl structure, a = 0.637 nm) [28, 30], reorganization of the crystal lattice must take place during the deposition of lithium. As the β phase has more open structure than the α phase, which is basically an expanded crystal lattice of aluminium, the reorganization during lithium deposition would create defects and enhance the diffusion rate of lithium in the process known as reactive crystallization. Thus, the formation of the β phase at the bulk of the electrode is essential for the development of the anode, as it will hold the electrode together, create extra surface for diffusion due to the expansion of the electrode and provide fast diffusion path within the extending β phase due to the availability of defects made during reorganization of the crystal lattice at the advancing front of the α/β phase boundary.

3.5. *Effect of impurities*

Methyl acetate was found, as received, to contain water, methanol and traces of acetic acid, all of which are reactive towards lithium. Typical levels of these impurities are shown in Table 3, which indicate very high concentration of methanol (2%), acetic acid (0.7%) and water (0.4%). The conventional purifica-

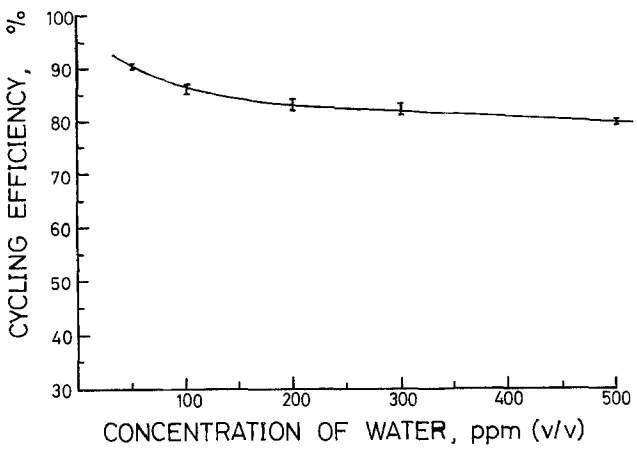

Fig. 7. The effect of water on cyling efficiency at steady state.

tion method of distillation under argon with lithium wire was found not to be sufficient to bring the concentrations down to acceptable levels (Table 3). Thus, a comprehensive treatment procedure was used to remove these impurities, which involved treatment with K_2CO_3 and acetic anhydride to remove methanol and acidic impurities, and the use of P_2O_5 to reduce the water content. Detailed procedure was given in the experimental section. The efficacy of this procedure is clearly demonstrated in Table 3, as the impurity levels are all brought down to below 0.01%.

A trace amount of water is shown to have a pronounced effect on alkali metal deposition [18, 31, 32] and as it is always present due to the unavoidable, though small leakage of the room air into the system, a detailed investigation of the effect of water on the cycling efficiency of the LiAl anode was conducted. The results are shown in Fig. 7. Under the cycling conditions of 5 mA cm^{-2} c.d. and 0.5 C cm^{-2} charge density, the cycling efficiency was found to increase with decreasing water levels. It increases rapidly above 90% when the water concentration falls below 50 ppm. For higher water concentrations, the change of the cyclic efficiency was small and it plateaud above 300 ppm water.

To quantify the interaction of lithium alloys with water, a standing corrosion test was devised for the calculation of the capacity loss rate by corrosion. The test involves, after the charging cycle, the addition of

Table 3. The levels of impurities in methyl acetate before and after purification

Impurities	*Before treatment*	*After treatment*	
		Distillation zone	*Comprehensive purification*
Methanol	2%	0.4%	< 0.01%
Acetic acid	0.7%	0.4%	< 0.01%
Water	0.4%	0.03%	< 0.01%

an open circuit standing period of 30 min before the discharging cycle. The loss in capacity is expressed in current units as shown in the following formula

$$i_{corr} = \frac{i_a(t_a - t'_a)}{t_p}$$

where i_{corr} = the capacity loss current density in mA cm^{-2}; i_a = the stripping current density in mA cm^{-2}; t_p = the standing time for the electrode under the open circuit condition in s; t_a = the time required to strip away the deposited lithium immediately after the plating process in s; t'_a = the time required to strip away the deposited lithium after the electrode was stood open circuit for a period of time t_p in s.

As 30 min was taken as the standing time, the i_{corr} is an average value of the corrosion rate within this period of time. Although the values obtained are not absolute, they give a general idea of the corrosion rate of the system. It is very useful for comparison purposes as one can calculate the relative percentage of the corrosion current to the charge and discharge currents.

The effect of water on the capacity loss rate is shown in Fig. 8. In general, the capacity loss rate is found to increase with increasing concentration of water in methyl acetate. However, the capacity loss rate falls rapidly at low water concentrations (< 50 ppm) and flattens off at high concentrations (> 300 ppm). The same trend was observed for the effect of water on the cycling efficiency (Fig. 7). This suggests that the determination of the cycling efficiency is to a large extent dependent on the corrosion powers of the solvent and its impurities.

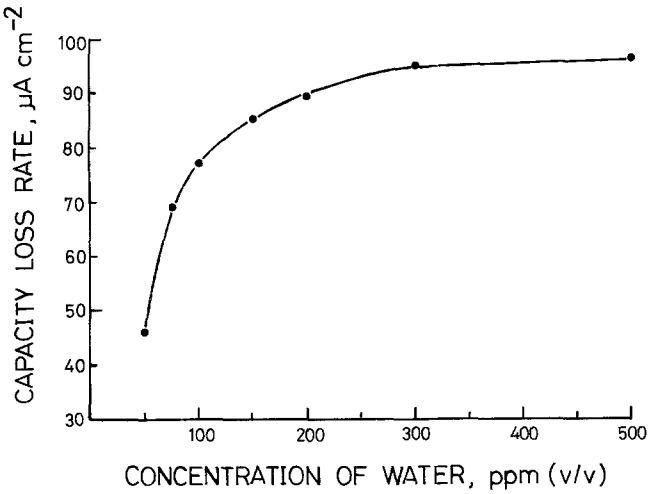

Fig. 8. The effect of water on the capacity loss rate.

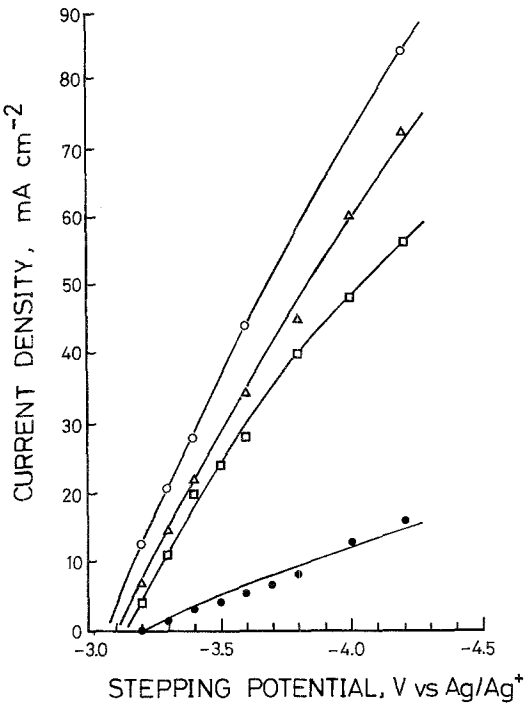

Fig. 9. The effect of supporting electrolytes on the current–potential curves obtained by the potential step method. Working electrode: Al, 0.13 cm^2. ○ 1 M $LiAsF_6$/MA, △ 1 M $LiPF_6$/MA, □ 1 M $LiClO_4$/MA, ● 1 M $LiBF_4$/MA.

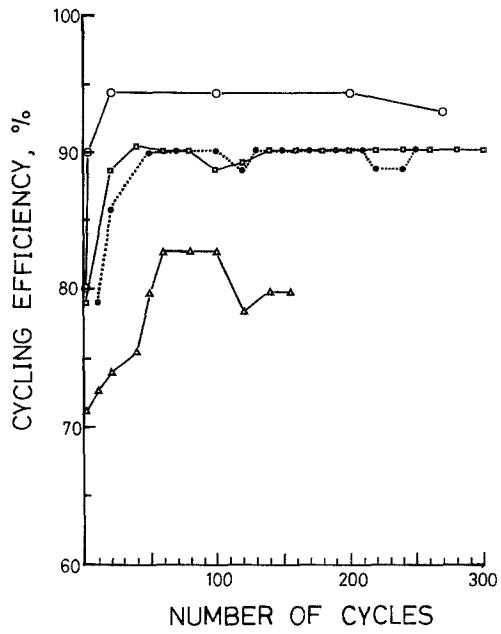

Fig. 10. The effect of supporting electrolytes on the cycling efficiency. Working electrode: Al, 0.13 cm^2; c.d.: 5 mA cm^{-2}. ○ 1 M $LiAsF_6$/MA, □ 1 M $LiClO_4$/MA, ● 1 M $LiBF_4$/MA, △ 1 M $LiPF_6$/MA.

3.6. *Effect of the supporting electrolytes*

Four commonly used supporting electrolytes such as $LiClO_4$, $LiAsF_6$, $LiPF_6$ and $LiBF_4$ were chosen to study their application in methyl acetate using the potential step method. The diffusion-controlled currents measured under potentiostatic conditions for equimolar concentrations of the various supporting electrolytes were found to follow the sequence: $LiAsF_6$ > $LiPF_6$ > $LiClO_4$ > $LiBF_4$ (Fig. 9). This sequence follows the same trend as the conductivity of the electrolytes (Table 4). In addition to having a higher conductance, $LiAsF_6$ was also shown to yield a high and stable coulombic efficiency at about 95% upon cycling (Fig. 10). The cycling stabilities of $LiClO_4$ and $LiBF_4$ are more or less the same, both at about 90%. Although $LiPF_6$ has a fairly high conductivity, the cycling efficiency is the lowest, between 70 and 80%. This may be due to the inherent instability of $LiPF_6$ [33]; colouration of the electrolyte was observed towards the end of the cycling test.

The interaction of the electrolyte with the lithium anode was studied using the standing corrosion test method as described in Section 3.5. The results are given in Table 5. The water content was kept to the same level, as far as possible, to assist comparison and their actual concentrations are given in Table 5 for reference. The same trend was again observed, indicating that the chemical reactivity between the electrolyte and the lithium anode may be the cause for the deterioration of the cycling efficiency. The results indicate that 1 M $LiAsF_6$ is clearly outstanding, as compared to the rest, in terms of corrosion resistance, as the capacity loss rate is only 0.26% of the plating current. This is in marked contrast to the other electrolytes. It should also be noted that the development of the electrodes occurred in the initial few cycles during which the cycling efficiency rose from low to steady values for all the supporting electrolytes used in the present studies (Fig. 10).

4. Conclusions

The following conclusions can be drawn from the work performed.

(1) Methyl acetate is a potential solvent for use in the ambient temperature lithium secondary battery, as it is cheap, readily available, easy to purify and can provide a high cycling efficiency of 95% and low

Table 4. Conductivities of supporting electrolytes in methyl acetate

Electrolytes	*Concentration (M)*	*Conductivity ($ohm^{-1} cm^{-1}$)*
$LiAsF_6$	1	0.0171
$LiPF_6$	1	0.0164
$LiClO_4$	1	0.00657
$LiBF_4$	1	0.00315

Table 5. The effect of supporting electrolytes on the capacity loss rates. Plating charge density = 0.5 C cm^{-2}. Plating current density, i_p = 5 mA cm^{-2}, stripping current density = 5 mA cm^{-2}

Supporting electrolytes	*Concentration of water (ppm)*	*i_c, capacity loss rates ($\mu A\ cm^{-2}$)*	i_c/i_p
1 M $LiAsF_6$	90	13	0.0026
1 M $LiClO_4$	100	77	0.015
1 M $LiBF_4$	90	85	0.017
1 M $LiPF_6$	80	480	0.096

capacity loss current (0.26% of the plating current) when using $LiAsF_6$ as the supporting electrolyte.

(2) $LiAsF_6$ is shown to be the best electrolyte to use due to its high conductivity and stability to corrosion effects in methyl acetate.

(3) The levels of impurities and water should be reduced to acceptable levels by the use of the purification procedures employed in the present study.

(4) Water is shown to have a deleterious effect on the cycling efficiency, which increases rapidly when the water level is low (< 50 ppm) and flattens off at higher water concentrations (> 300 ppm).

(5) The development of the LiAl anode is indicated by the decrease in the nucleation polarization of the β phase, the reduction in the concentration polarization during charge and discharge, and the more ready acceptance of lithium by the developed electrode. This development also leads to the expansion of the external morphology of the electrode and the formation of a radiative structure of the LiAl alloys to the interior of the electrode.

(6) The optimum conditions for maximum cycling efficiency are found at a current density of $5\,mA\,cm^{-2}$ and a charge density of $0.5\,C\,cm^{-2}$.

Acknowledgement

We thank the Research Grant Committee of the Hong Kong University for their continued support for the lithium battery project.

References

[1] A. S. Baranski and W. R. Fawcett, *J. Electrochem. Soc.* **129** (1982) 901.
[2] A. N. Dey, *J. Electrochem. Soc.* **118** (1971) 1547.
[3] R. Selim and P. Bro, *J. Electrochem. Soc.* **121** (1974) 1457.
[4] R. D. Rauh, T. F. Reise and S. B. Brummer, *J. Electrochem. Soc.* **125** (1978) 186.
[5] R. D. Rauh and S. B. Brummer, *Electrochim. Acta* **22** (1977) 75.
[6] S. G. Meibuhr, *J. Electrochem. Soc.* **117** (1970) 56.
[7] V. R. Koch and S. B. Brummer, *Electrochim. Acta* **23** (1978) 55.
[8] E. J. Frazer, *J. Electroanal. Chem.* **121** (1981) 329.
[9] I. Epelboin, M. Froment, M. Garreau, J. Thevenin and D. Warin, *J. Electrochem. Soc.* **127** (1980) 2100.
[10] S. I. Tobishima and T. Okada, *J. Applied Electrochem.* **15** (1985) 317.
[11] G. H. Newman, R. W. Francis, L. H. Gaines and B. M. L. Rao, *J. Electrochem. Soc.* **127** (1980) 2025.
[12] T. R. Jow and C. C. Liang, *J. Electrochem. Soc.* **129** (1982) 1429.
[13] A. N. Dey and E. J. Rudd, *J. Electrochem. Soc.* **121** (1974) 1294.
[14] V. R. Koch, *J. Electrochem. Soc.* **126** (1979) 181.
[15] V. R. Koch and J. H. Young, *J. Electrochem. Soc.* **125** (1978) 1371.
[16] J. L. Goldman, R. M. Mank, J. H. Young and V. R. Koch, *J. Electrochem. Soc.* **127** (1980) 1461.
[17] P. G. Glugla, *J. Electrochem. Soc.* **130** (1983) 113.
[18] R. D. Rauh and S. B. Brummer, *Electrochim. Acta* **22** (1977) 85.
[19] F. W. Dampier and S. B. Brummer, *Electrochim. Acta* **22** (1977) 1339.
[20] J. S. Foos and J. McVeigh, *J. Electrochem. Soc.* **130** (1983) 628.
[21] V. R. Koch, *J. Power Souces* **6** (1981) 357.
[22] S. B. Brummer, 'Extended Abstracts', Int. Meeting on Lithium Batteries, Rome, Italy, No. 1 (1982).
[23] F. D. Dousek, J. Jansta and J. Riha, *J. Electroanal. Chem.* **46** (1973) 281.
[24] M. W. Rupich, L. Pitts and K. M. Abraham, *J. Electrochem. Soc.* **129** (1982) 1857.
[25] J. O. Besenhard, *J. Electroanal. Chem.* **94** (1978) 77.
[26] H. C. Lai, Electrochemical Studies of the Lithium-Aluminium Anode in Methyl Acetate, M. Phil. Thesis, University of Hong Kong (1986).
[27] J. O. Besenhard and G. Eichinger, *J. Electroanal. Chem.* **68** (1976) 1.
[28] R. P. Elliott, 'Constitution of Binary Alloys', 1st supplement, McGraw-Hill, New York (1965) p. 42.
[29] M. Hansen, 'Constitution of Binary Alloys', McGraw-Hill, New York (1958) pp. 104–105.
[30] F. A. Shunk, 'Constitution of Binary Alloys', 2nd supplement, McGraw-Hill, New York (1969) pp. 27–28.
[31] G. Nazri and R. H. Muller, *J. Electrochem. Soc.* **132** (1985) 2050.
[32] J. R. Selman, D. K. DeNuccio, C. J. Sy and R. K. Steunenberg, *J. Electrochem. Soc.* **124** (1977) 1160.
[33] J. R. Wasson and D. K. Hoffman, 'Proc. Symp. on Power Sources for Biomedical Implantable Applications and Ambient Temp. Lithium Batteries' (1980) Vol. 80-4, p. 309.